VOLUME 10 NUMBER 6 JUNE 2007
www.nature.com/natureneuroscience

nature neuroscience

Acoustic flutter in auditory cortex

Identifying the olfactory neural stem cell

Increased connectivity in synesthesia

nature neuroscience

Differential neural coding of acoustic flutter within primate auditory cortex

Daniel Bendor & Xiaoqin Wang

A sequence of acoustic events is perceived either as one continuous sound or as a stream of temporally discrete sounds (acoustic flutter), depending on the rate at which the acoustic events repeat. Acoustic flutter is perceived at repetition rates near or below the lower limit for perceiving pitch, and is akin to the discrete percepts of visual flicker and tactile flutter caused by the slow repetition of sensory stimulation. It has been shown that slowly repeating acoustic events are represented explicitly by stimulus-synchronized neuronal firing patterns in primary auditory cortex (AI). Here we show that a second neural code for acoustic flutter exists in the auditory cortex of marmoset monkeys (*Callithrix jacchus*), in which the firing rate of a neuron is a monotonic function of an acoustic event's repetition rate. Whereas many neurons in AI encode acoustic flutter using a dual temporal/rate representation, we find that neurons in cortical fields rostral to AI predominantly use a monotonic rate code and lack stimulus-synchronized discharges. These findings indicate that the neural representation of acoustic flutter is transformed along the caudal-to-rostral axis of auditory cortex.

A fundamental role of the auditory system is to encode the time-varying structure of an acoustic signal. Acoustic events, such as a brief sound or a transient change in amplitude or frequency within an acoustic signal, repeat quasi-periodically at a specific rate for many natural and biologically relevant sounds[1,2]. For repetitions of an acoustic event at rates between approximately 10 and 45 Hz, such as the tapping sound produced by a woodpecker, we hear a discretely sounding percept known as acoustic flutter[3–5] (**Supplementary Audio 1** online). Slow repetition rates (or modulation frequencies) in this range are important for identifying consonants and understanding sentences in speech[6], as well as for the phrasing of many animal vocalizations (such as a marmoset's trill call)[7,8]. Repetition rates above the upper limit of the flutter percept can generate a pitch, which is a more continuous sounding percept than flutter[4,5] (**Supplementary Audio 2** online). For repetition rates below the lower limit of flutter we no longer perceive a repetition rate, but instead hear individual acoustic events that occur distinctly in time[3] (**Supplementary Audio 3** online).

Slow repetition rates in an acoustic signal (in the range of acoustic flutter) are represented explicitly in AI by a subpopulation of neurons that can synchronize their spike timing to each acoustic event[9]. Faster repetition rates, above the perceptual range of flutter, are encoded by the discharge rates of a different neuronal population that does not synchronize to repeated acoustic events and contains no information about repetition rate in its temporal discharge patterns[10,11]. Given that AI neurons generally cannot synchronize to stimulus repetitions at fast rates[10], a neural code based on discharge rate rather than spike timing explains why we can still discriminate and perceive these repetition rates. However, if slow repetition rates are encoded by the temporal pattern of neuronal firing (which explicitly represents when each acoustic event occurs), are discharge rates used in parallel to encode the repetition rate of the acoustic signal? Even if AI neurons only use spike timing to encode slow repetition rates, stimulus synchronization seems to be poorer in cortical areas outside AI[12], and auditory cortex might therefore have to use discharge rate to encode slow repetition rates that cannot be represented temporally.

In the somatosensory system, the frequency of tactile vibration (analogous to the repetition rate of acoustic signals) is differentially encoded by distinct neural populations in primary somatosensory cortex, such that rapidly adapting neurons encode low-frequency vibration (flutter) whereas pacinian neurons encode high-frequency vibration[13]. The neural encoding boundary between these two populations occurs near a vibration frequency of approximately 40 Hz, which is close to the encoding boundary between the temporal and rate-coding populations in AI (of awake marmoset monkeys)[10]. Furthermore, for both the auditory and somatosensory systems, this neural encoding boundary also matches the perceptual discrete/continuous boundary for a sequence of sensory events[4,5,13,14]. Given these similarities, we hypothesized that other aspects of the way in which the percept of flutter is encoded in somatosensory cortex might also be found in auditory cortex.

Previous work has shown that temporal information from spike timing in rapidly adapting neurons was sufficient to determine the frequency of tactile vibration[15–17]. More recently, another group found a second neural code in a subset of rapidly adapting neurons, in the form of a discharge rate that increases monotonically as a function of vibration frequency over the perceptual range of flutter[18,19]. Although

Laboratory of Auditory Neurophysiology, Department of Biomedical Engineering, Johns Hopkins University School of Medicine, 720 Rutland Avenue, Traylor Building 412, Baltimore, Maryland 21205, USA. Correspondence should be addressed to D.B. (dbendor@jhu.edu) or X.W. (xiaoqin.wang@jhu.edu).

Received 31 January ; accepted 7 March; published online 29 April 2007; doi:10.1038/nn1888

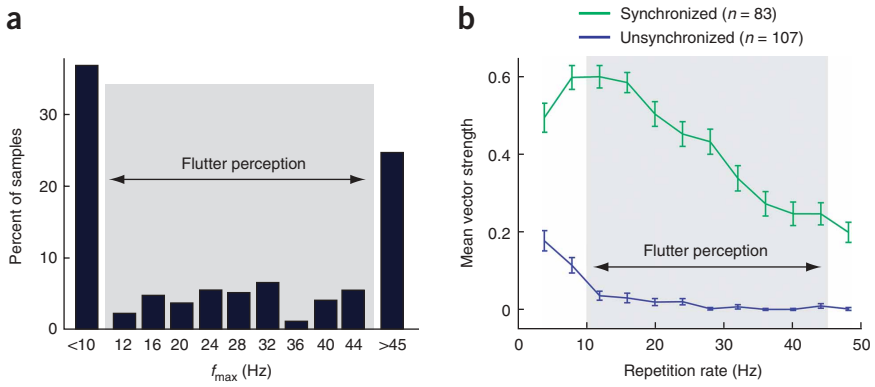

Figure 1 Stimulus synchronization to acoustic pulse trains. (**a**) Distribution of the repetition rate limit for stimulus-synchronized discharges (f_{max}) for all neurons in this study. Of the neurons tested with repetition rates between 4–10 Hz, 58% (50/86) did not synchronize to the stimulus, 16% (14/86) synchronized at 4 Hz, and 26% (22/86) synchronized at 8 Hz. $n = 274$. (**b**) Population average vector strength of synchronized (green) and unsynchronized (blue) neurons. Error bars represent s.e.m.

neurons in primary somatosensory cortex (S1) have a dual temporal/rate representation of flutter, secondary somatosensory cortex (S2) encodes flutter using only a monotonic rate code, and lacks the stimulus-synchronized discharges observed in S1 (refs. 18,20). Rate codes, in which the discharge rate is a monotonic function of a stimulus parameter, are not unique to the somatosensory system and have also been reported in both the visual and auditory systems[21–23]. Monotonic rate codes are typically not narrowly tuned, and thus might encode information by their response function's slope rather than its peak. Theoretical studies have shown that the slope of a neuron's tuning function can have an important role in coding sensory stimuli[24,25].

Auditory cortex contains two main regions: the core region responds to spectrally narrowband sounds and the belt region to wideband sounds[26,27]. The core and belt regions are further divided into multiple fields, each with its own cochleotopic representation[26–28]. In this study we have focused our recordings on the three core fields: AI (primary auditory cortex), R (rostral field) and RT (rostral temporal field). Fields AI, R and RT share reciprocal connections with the ventral division of the medical geniculate body (vMGB) as well as with each other (although the connections between AI and RT are more limited)[26]. Little is known about the physiological properties of field RT, whereas several differences between R and AI have been observed, most notably a slightly longer (~10 ms) response latency in field R[29]. Along the medial-to-lateral axis of the superior temporal gyrus (starting from AI), the spectral preference of neurons changes from narrowband to wideband[27,30,31], and it has been postulated that cortical fields have similar spectral preferences along the caudal-to-rostral axis[26]. In this study, we have compared the neural encoding properties of the three core fields (AI, R, and RT) aligned along the caudal-to-rostral axis of the superior temporal gyrus. Our findings indicate that acoustic flutter is encoded differently along the caudal-to-rostral axis of auditory cortex: AI contains a dual temporal/rate representation whereas cortical fields rostral to AI predominantly use a monotonic rate code that is unsynchronized to acoustic flutter.

RESULTS

We recorded from the auditory cortex of four awake marmoset monkeys a total of 274 well-isolated single neurons that responded significantly, either by stimulus synchronization and/or discharge rate (see Methods), to acoustic pulse trains spanning the perceptual range of acoustic flutter. The most common stimulus set used in these experiments had a repetition rate that varied linearly in 4-Hz intervals between 4 and 48 Hz (see Methods). The acoustic pulse trains used in these experiments were sequences of brief tone or noise bursts (**Supplementary Fig. 1** online) centered at the neuron's characteristic frequency (CF). Neurons generally could synchronize at repetition rates near the upper limit of flutter (~45 Hz) or could not synchronize to any of the repetition rates tested that were above the lower limit of flutter (~10 Hz; **Fig. 1a**), which is consistent with previous studies of stimulus synchronization in the auditory cortex of awake marmosets[10]. Based on these results, we classified neurons into one of three groups according to their ability to synchronize (Rayleigh test, $P < 0.001$) to repetition rates within the flutter range: synchronized (107/274), mixed response (29/274) and unsynchronized (138/274). Synchronized neurons typically had short-latency responses with stimulus-synchronized discharges up to a stimulus repetition rate of at least 40–50 Hz. Unsynchronized neurons typically had longer-latency responses than synchronized neurons, and generally did not show significant stimulus synchronization at repetition rates above 10 Hz (**Fig. 1b**). Some unsynchronized neurons could synchronize at repetition rates below 10 Hz, and therefore our use of the term 'unsynchronized' refers only to neuronal responses at repetition rates within the perceptual range of flutter. All unsynchronized neurons and most synchronized neurons (92/107) had significant discharge rates for at least a subset of acoustic pulse trains with repetition rates within the

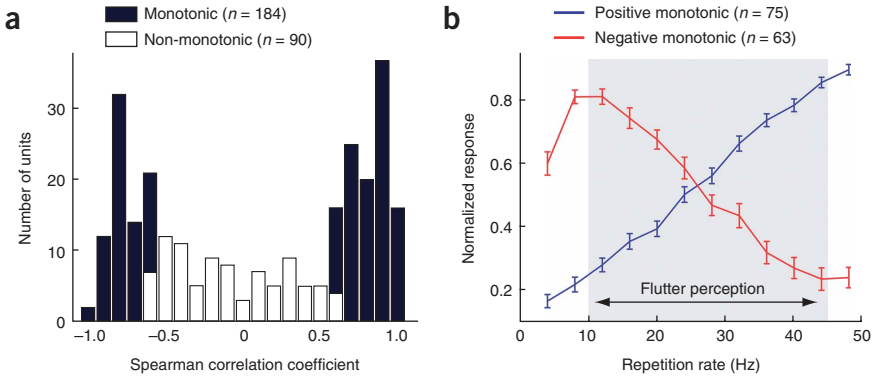

Figure 2 Monotonic response properties. (**a**) Distribution of the Spearman correlation coefficient for neurons with monotonic (filled bars) and non-monotonic (unfilled bars) response functions of repetition rate. Spearman correlation coefficients of 1 and –1 have perfect positive and negative monotonicity, respectively. Neurons with a statistically significant Spearman correlation coefficient ($P < 0.05$) are considered monotonic. (**b**) Normalized discharge rates for positive (blue) and negative (red) monotonic neurons. This figure includes data from all synchronized, mixed and unsynchronized neurons. Only data collected with stimulus set 1 (see Methods) are shown. Error bars represent s.e.m.

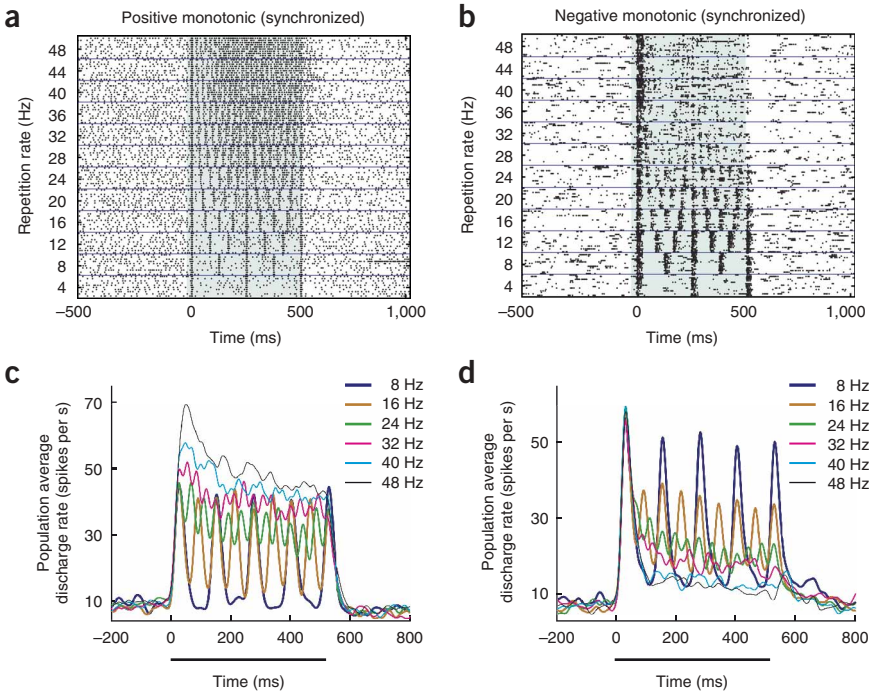

Figure 3 Examples of positive and negative monotonic synchronized responses. (**a**) Raster plot of a positive monotonic synchronized neuron's response (unit M2P-785) for repetition rates between 4 and 48 Hz. This neuron had a significant vector strength (Rayleigh test, $P < 0.001$) over the entire range of repetition rates. The shaded portion of the plot indicates the time period when the acoustic stimulus was played. (**b**) Raster plot of a negative monotonic synchronized neuron's response (unit M32Q-46) for repetition rates between 4 and 48 Hz. This neuron had a significant vector strength (Rayleigh test, $P < 0.001$) over the entire range of repetition rates. (**c**,**d**) Instantaneous discharge rates plotted over the duration of the stimulus for positive (**c**; $n = 22$) and negative (**d**; $n = 29$) monotonic synchronized neurons. The bar underneath the plot indicates the time period when the acoustic stimulus was played. Only data collected with stimulus set 1 (see Methods) are shown.

range of flutter perception. Several neurons in our study could be classified as synchronized or unsynchronized depending on sound level or acoustic pulse duration, and we refer to these as having a mixed response.

Prevalence of monotonic rate coding

Next, we investigated whether the discharge rates of neurons varied as a monotonic function of repetition rate over the perceptual range of flutter. We quantified monotonicity by calculating the Spearman correlation coefficient between discharge rate and repetition rate (see Methods). Our justification for quantifying monotonicity by measuring correlation non-parametrically (as opposed to fitting the data to a function) is that this method does not assume a linear or sigmoidal relationship between discharge rate and repetition rate. Roughly two-thirds of the sampled neurons (184/274) increased or decreased their discharge rate monotonically as a function of repetition rate (Spearman correlation coefficient, $P < 0.05$; **Fig. 2a**). We refer to these two response types as 'positive monotonic' and 'negative monotonic', respectively. The average discharge rates of positive (negative) monotonic responses increased (decreased) linearly with increasing repetition rate over the range associated with flutter perception (**Fig. 2b**, **Supplementary Fig. 2** online).

Of 107 synchronized neurons, 34 neurons increased and 33 neurons decreased their discharge rate monotonically as a function of repetition rate (**Fig. 3**). Around two-thirds of the unsynchronized population

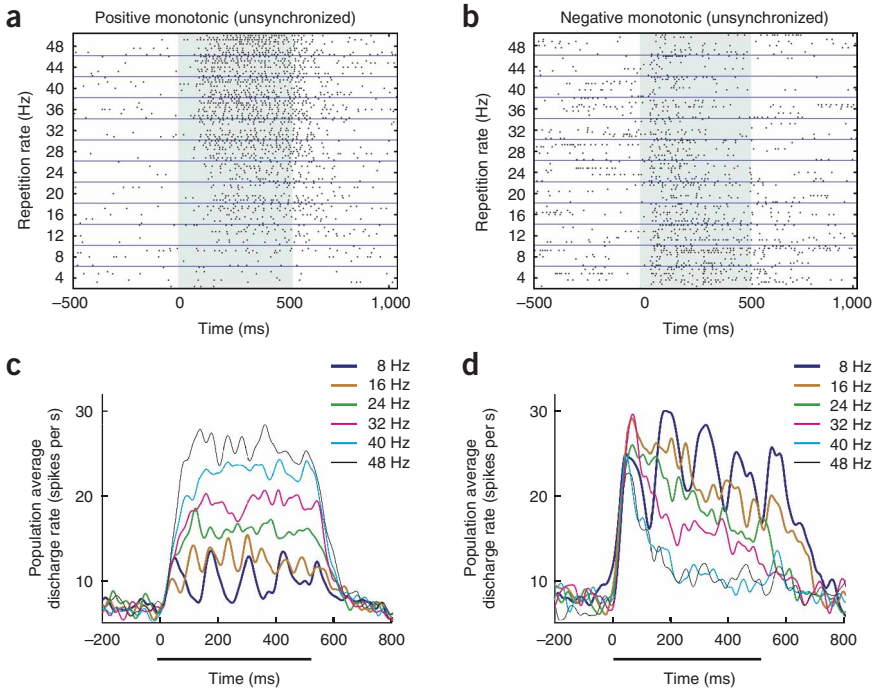

Figure 4 Examples of positive and negative monotonic unsynchronized responses. (**a**) Raster plot of a positive monotonic unsynchronized neuron's response (unit M32Q-210) for repetition rates between 4 and 48 Hz. The neuron did not show significant stimulus synchronization at any of the repetition rates tested. The shaded portion of the plot indicates the time period when the acoustic stimulus was played. (**b**) Raster plot of a negative monotonic unsynchronized neuron's response (unit M2P-388) for repetition rates between 4 and 48 Hz. The neuron did not show significant stimulus synchronization at any of the repetition rates tested. (**c**,**d**) Instantaneous discharge rates plotted over the duration of the stimulus for positive (**c**; $n = 47$) and negative (**d**; $n = 25$) monotonic unsynchronized neurons. The bar underneath the plot indicates the time period when the acoustic stimulus was played. Only data collected with stimulus set 1 (see Methods) are shown.

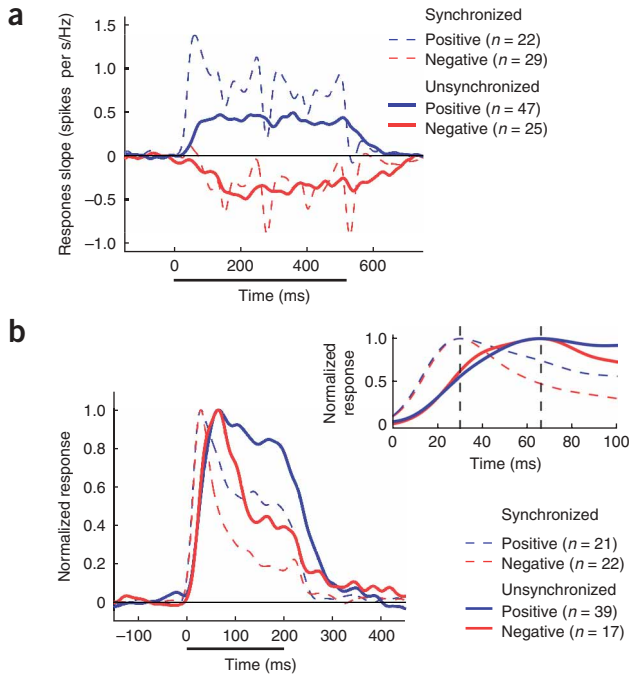

Figure 5 Temporal response dynamics of synchronized and unsynchronized neurons. (**a**) Changes in the instantaneous response slope for synchronized (dashed lines) and unsynchronized (solid lines) neurons with positive (blue) or negative (red) monotonic responses, obtained by linear interpolation of the mean population neuronal responses (shown in **Fig. 3c,d** and **Fig. 4c,d**) across all repetition rates between 8 and 48 Hz. The bar underneath the plot indicates the time period when the acoustic stimulus was played. (**b**) Normalized population PSTH of synchronized and unsynchronized neurons with positive and negative monotonic responses for a pure tone at the sound level eliciting the maximum discharge rate. The inset shows a magnified version of the plot for the first 100 ms of the response. Peak latencies were 31 ms for the positive monotonic synchronized population, 30 ms for the negative monotonic synchronized population, and 63 ms for both the positive and negative monotonic unsynchronized populations. Synchronized and unsynchronized populations with a similar direction of monotonicity had statistically significant differences in peak latencies (Wilcoxon rank sum test, positive monotonic: $P < 5.0 \times 10^{-4}$, negative monotonic: $P < 5.0 \times 10^{-3}$). The bar underneath the plot indicates the time period when the acoustic stimulus was played.

(91/138) had discharge rates that varied as either a positive ($n = 61$) or a negative ($n = 30$) monotonic function of repetition rate over the perceptual range of flutter (**Fig. 4**, **Supplementary Fig. 3** online). In addition to neurons with strictly synchronized or unsynchronized responses, we recorded 29 neurons that switched between stimulus-synchronized and unsynchronized responses (with significant discharge rates) depending on the sound level or pulse width of the acoustic stimulus. These neurons were classified as having a mixed response, and were analyzed separately from the synchronized and unsynchronized neuronal populations. Most of these neurons (25/29) had discharge rates that varied as a monotonic function of repetition rate (**Supplementary Table 1** online).

Although the slopes of monotonic responses were generally either strictly positive or negative across different acoustic signals, we found a few examples ($n = 4$) of neurons that switched between positive and negative monotonic responses, depending on the sound level or carrier frequency used (**Supplementary Table 1**).

The neurons that did not show a significant monotonic relationship between discharge rate and repetition rate were classified as 'non-monotonic' (**Fig. 2a**). Although positive and negative monotonic responses were fairly homogenous, there were several different types of non-monotonic response (**Supplementary Fig. 4** online). The most common non-monotonic responses were all-pass, in which discharge rate varied minimally with repetition rate over the perceptual range of flutter (**Supplementary Fig. 4a**). We also observed bandpass, low-pass, high-pass and multi-peak (complex) responses (**Supplementary Fig. 4b–e**).

Comparison of synchronized and unsynchronized responses

We found monotonic responses in both synchronized and unsynchronized neurons. If synchronized neurons contain additional information about the acoustic stimulus in their temporal firing patterns, does the loss of stimulus-synchronized discharges provide a neural coding advantage for unsynchronized neurons? Because of stimulus synchronization, discharge rate measured over a short time window fluctuates rapidly during the acoustic stimulus (**Fig. 3c,d**). As such, a synchronized neuron's response slope — the linear relationship between discharge rate and repetition rate (see Methods) — becomes an unreliable description of the acoustic signal's repetition rate when calculated over short time windows. However, unsynchronized neurons lack stimulus synchronization (**Fig. 4c,d**) and, as such, can provide similar monotonic response slopes throughout the duration of the stimulus. We compared the temporal dynamics of the response slopes of monotonic synchronized and unsynchronized neurons over the time course of the stimulus (**Fig. 5a**). Unsynchronized neurons showed much less variation in their response slope during the stimulus

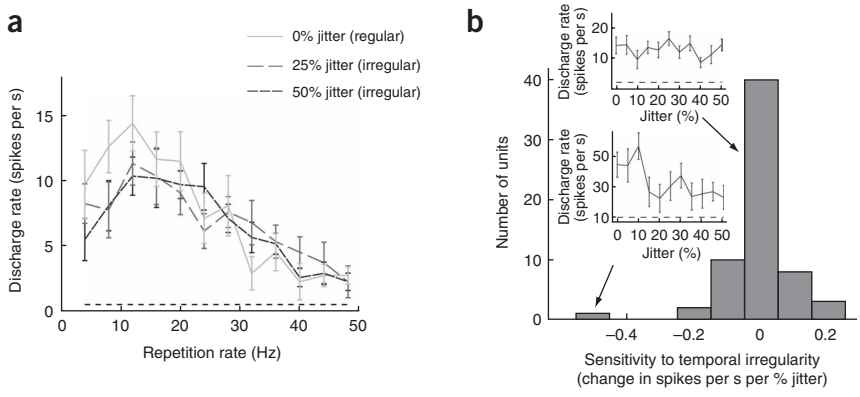

Figure 6 Flutter rate codes are insensitive to temporal irregularity. (**a**) Repetition rate tuning of a negative monotonic unsynchronized neuron (unit M41O-306) for regular (0% jitter) and irregular (25% and 50% jitter) acoustic pulse trains. The dashed black line indicates the significance level for discharge rate (2 s.d. away from the spontaneous discharge rate). (**b**) Distribution of the interpolated change in discharge rate per % jitter for 64 neurons: synchronized ($n = 25$), mixed ($n = 11$) and unsynchronized ($n = 28$). These neurons were located in AI ($n = 23$) or the rostral fields ($n = 37$), or were on the border or outside the core fields ($n = 4$). Both monotonic ($n = 48$) and non-monotonic ($n = 16$) response types were included here. Insets show two examples of an unsynchronized neuron's response to irregular pulse trains: jitter insensitivity in a monotonic neuron (unit M32Q-217; top) and jitter sensitivity in a neuron with a non-monotonic response to repetition rate (unit M2P-404; bottom). Error bars represent s.e.m.

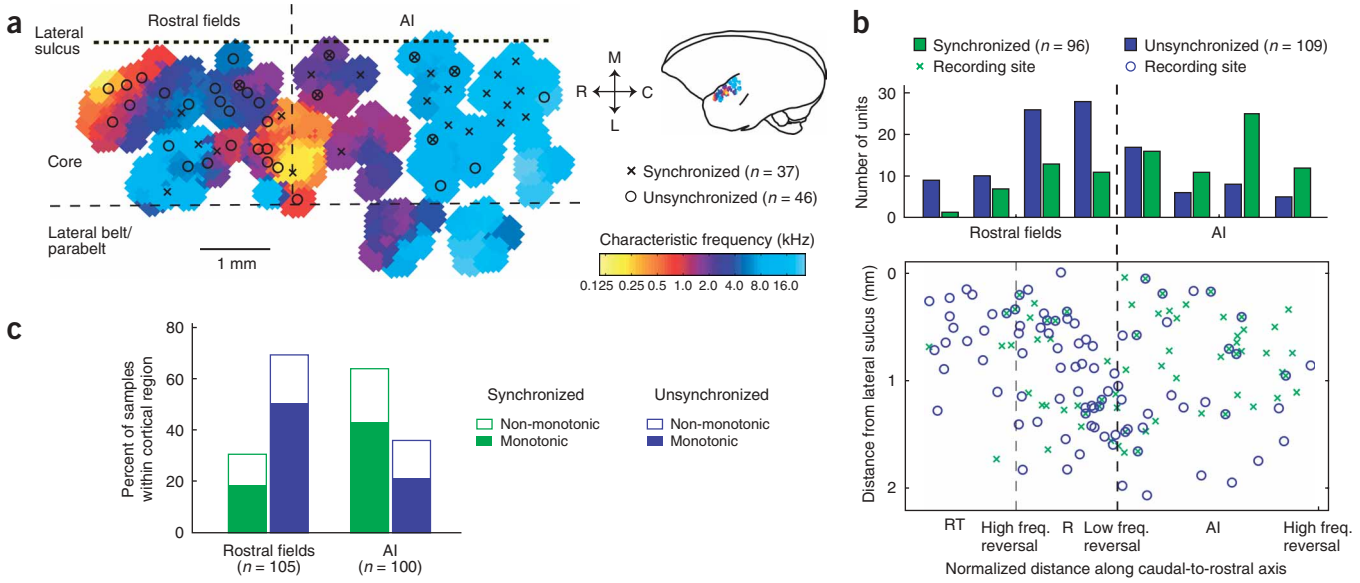

Figure 7 Comparison of the proportion of response types by cortical region. (**a**) Cortical frequency map from one subject (M32Q, left hemisphere), with the recording sites of synchronized (crosses) and unsynchronized (circles) neurons indicated. The upper right portion of the figure shows a diagram of the marmoset's brain and the location of the cortical map. R, rostral; C, caudal; M, medial; L, lateral. (**b**) A normalized cortical map for four hemispheres (three left, one right). Normalized recording site positions are indicated for synchronized (crosses) and unsynchronized (circles) neurons. A histogram showing the spatial distribution for these two neuron types is shown above the map. Green, synchronized; blue, unsynchronized. (**c**) Comparison of the proportion of monotonic and non-monotonic responses to repetition rate for synchronized and unsynchronized neurons in AI and the rostral fields (R, RT). Green, synchronized; blue, unsynchronized. Filled bar, monotonic; unfilled bar, non-monotonic.

than did synchronized neurons (**Fig. 5a**), thus providing a temporally more stable monotonic rate code for repetition rate. Neurons with unsynchronized responses had significantly longer latencies in their peak responses to pure tones than neurons with synchronized responses (**Fig. 5b**), indicating that this neural coding advantage might cause these neurons to incur a processing time cost.

Periodicity is not encoded by discharge rate

In humans, average discrimination thresholds for repetition rate are similar for periodic and aperiodic acoustic pulse trains with low repetition rates[32]. At higher repetition rates (in the range of pitch perception), average repetition rate discrimination worsens for aperiodic pulse trains[32]. To determine whether the discharge rate-based representation of flutter was sensitive to changes in the temporal regularity of the stimulus, we compared the neuronal responses evoked by regular and irregular pulse trains. A representative example of an unsynchronized neuron's response function to repetition rate for both regular and irregular pulse trains is shown in **Figure 6a**. This neuron showed similar negative monotonic responses for regular and irregular acoustic pulse trains. Irregular pulse trains were generated by temporally shifting each acoustic transient in a regular pulse train by an amount randomly selected from a uniform distribution (see Methods). The temporal irregularity in the pulse train was increased parametrically, without affecting the average repetition rate, by expanding the width of this uniform distribution. For example, the maximum temporal jitter for a pulse train with a repetition rate of 20 Hz (50 ms interpulse interval) ranged from ±2.5 ms (5% maximum jitter) to ±25 ms (50% maximum jitter). The change in discharge rate between regular and maximally irregular pulse trains (50% jitter), determined using linear interpolation, was less than 5 spikes per s for roughly 81% (52/64) of the neurons tested. Although a few neurons did show some sensitivity to temporal irregularity (**Fig. 6b**, lower inset), most neurons tested with irregular pulse trains showed little variation in their discharge rates (**Fig. 6b**). We found no significant effect on the sensitivity to temporal irregularity resulting from either neuron type (synchronized or unsynchronized) or neuron location (Kolmogorov-Smirnov test, $P > 0.1$).

This finding indicates that neural encoding of flutter solely on the basis of discharge rate is largely insensitive to the acoustic signal's periodicity, and reflects the average repetition rate. This is in sharp contrast to the sensitivity for temporal irregularity observed in pitch-selective neurons, which are non-monotonically tuned to repetition rates above the range that generates a percept of flutter[33]. Human subjects can discriminate between a regular and irregular acoustic pulse train, although jitter detection thresholds are higher for repetition rates in the range of flutter compared to pitch[34]. Given that synchronized responses also occur for aperiodic pulse trains[10], the information contained in stimulus-synchronized discharge patterns could potentially be used by the auditory system to distinguish between periodic and aperiodic pulse trains.

Comparison of AI and the rostral core fields

We compared the spatial distribution of response types along the caudal-to-rostral axis of auditory cortex. The border between AI and the rostral core fields (R and RT) was identified by locating the reversal in the cochleotopic map between AI and R (**Fig. 7**, see Methods). This border was identified in the four hemispheres that we mapped (one hemisphere per monkey).

We found a higher proportion of synchronized neurons than unsynchronized neurons in AI, whereas in the rostral fields there was a higher percentage of unsynchronized neurons. An example of the recording site locations of these two neuron types from one cortical frequency map is shown in **Figure 7a**. Differences in the spatial distribution of synchronized and unsynchronized neurons were assessed by first creating a normalized map of recording sites across all four monkeys, based on the cochleotopic gradient (see Methods),

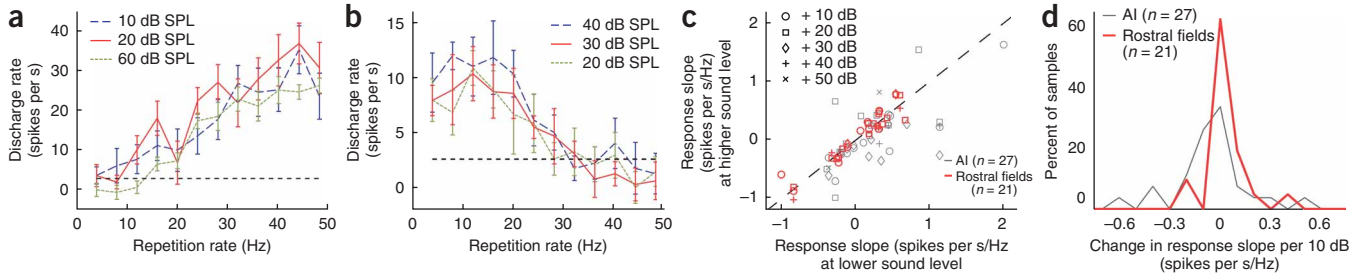

Figure 8 Sound-level invariance in monotonic rate-coding neurons. (**a**) Response of a positive monotonic unsynchronized neuron (unit M2P-921) to repetition rate across three sound levels (10, 20 and 60 dB sound pressure level (SPL)). The dashed black line indicates the significance level for discharge rate (2 s.d. away from the spontaneous discharge rate). (**b**) Response of a negative monotonic unsynchronized neuron (unit M32Q-141) to repetition rate across three sound levels (20, 30 and 40 dB SPL). (**c**) Comparison of the response slope for monotonic rate-coding neurons in AI (gray) and the rostral fields (red) at the minimum sound level tested, and a sound level 10–50 dB higher. (**d**) The change in response slope for a 10 dB increase in sound level for neurons in AI (gray) and the rostral fields (red). The distributions were significantly different (Kolmogorov-Smirnov test, $P < 0.02$) with a higher percentage of rostral field neurons having response slopes that changed by less than 0.05 per 10 dB.

and then comparing recording site locations along the caudal-to-rostral and medial-to-lateral axes. Synchronized and unsynchronized neurons showed significantly different spatial distributions (Wilcoxon rank sum test) along the caudal-to-rostral axis, parallel to the lateral sulcus ($P < 7.0 \times 10^{-7}$; **Fig. 7b**) but not along the medial-to-lateral axis perpendicular to the lateral sulcus ($P = 0.37$). Furthermore, there was no significant difference ($P = 0.59$) in the distribution of synchronized and unsynchronized neurons within AI along the caudal-to-rostral axis (neurons on the AI/R border were excluded from this analysis). Roughly two-thirds of the synchronized neurons were located in AI, whereas two-thirds of the unsynchronized neurons were located in the rostral fields (**Fig. 7c**, **Supplementary Table 1**). These proportions remained similar even if neurons near the AI/R border were excluded from the analysis (**Supplementary Table 1**). The difference in the spatial distributions along the caudal-to-rostral axis was still observed if we limited the comparison to synchronized and unsynchronized neurons with monotonic responses ($P < 1.5 \times 10^{-6}$). However, if the comparison was limited to the non-monotonic neurons, there was no longer a significant difference between the spatial distributions of synchronized and unsynchronized neurons along the caudal-to-rostral axis ($P = 0.09$). Therefore the change from a synchronized to an unsynchronized response between AI and the rostral fields occurred mainly in the monotonic population (**Fig. 7c**). Similar proportions of neurons with positive (54%) and negative (46%) monotonic responses were observed in the rostral fields, whereas most AI neurons ($\sim$70%) were positive monotonic (**Supplementary Table 1**).

Synchronized neurons in both AI and the rostral fields had stimulus-synchronized discharges over the entire frequency range of flutter (**Supplementary Fig. 5a** online). Unsynchronized neurons in both AI and the rostral fields did not synchronize within the range of flutter but had significant mean population vector strengths (Wilcoxon rank sum, $P < 0.01$) at repetition rates below the lower limit of flutter (**Supplementary Fig. 5b**). In the rostral fields, responses to pure tones were generally weaker and had longer peak latencies than in AI, for both the synchronized and unsynchronized neuronal populations (**Supplementary Fig. 5c**,**d**).

Effect of sound level on monotonic rate codes

The discharge rates of neurons in auditory cortex generally depend on the sound level[35], creating a potential ambiguity for a discharge rate-based representation of repetition rate. However, the response slopes of many of the neurons we studied were largely unaffected by moderate changes (10–50 dB) in sound level (**Fig. 8a**,**b**). We quantified the extent to which the response slope changed between sound levels that differed by 10–50 dB. Neurons in both AI and the rostral fields showed a significant correlation (Pearson correlation coefficient, AI: $r = 0.76$, $P < 4.9 \times 10^{-6}$; rostral fields: $r = 0.94$, $P < 3.4 \times 10^{-10}$) between their response slopes for pulse trains at two different sound levels (**Fig. 8c**). We next determined how much the response slope changed for a 10-dB increase in sound level using linear interpolation (see Methods). Significantly more neurons in the rostral fields than in AI varied their response slopes by less than 0.05 for a 10-dB sound level change (Kolmogorov-Smirnov test, $P < 0.02$; **Fig. 8d**). However, we found no significant difference in sound level-dependent changes in the response slope between synchronized, mixed and unsynchronized neurons (**Supplementary Fig. 6a**,**b** online; Kolmogorov-Smirnov test, $P > 0.1$).

The acoustic pulse trains used in these experiments were normalized for amplitude (relative to other pulse trains in the stimulus set), and as such acoustic signals with faster repetition rates had greater overall energy. Although neural discharge rates in auditory cortex generally depend on the energy level of the acoustic stimulus, neuronal response slopes were similar (Pearson correlation coefficient, $r = 0.81$, $P < 2.6 \times 10^{-8}$) for equal amplitude and energy-normalized pulse trains (**Supplementary Fig. 6c**).

DISCUSSION

How does the auditory system encode the repetition rate of acoustic flutter? Our results indicate that repetition rate is dually represented in AI by both the discharge rate and stimulus-synchronized firing patterns of neurons. In the rostral fields (R and RT), stimulus-synchronized activity is weaker, and unsynchronized responses to acoustic flutter are more common. Neurons in the rostral fields primarily use a rate code in which discharge rates either increase or decrease monotonically over the range of repetition rates associated with flutter perception. The monotonic rate coding of flutter represents the average repetition rate, as discharge rates generally do not vary significantly between periodic and aperiodic versions of the same acoustic pulse train. Although many monotonic neurons showed some degree of sound level invariance (over moderate changes in sound level), this was more common in neurons in the rostral fields.

The use of monotonic or slope-based rate coding in the auditory system is not unique for representing repetition rate, and has been reported in auditory cortex for encoding sound level[36] and source location[22]. The complementary coding (using opponent channels) of repetition rate using positive and negative, monotonically varying discharge rates might be advantageous in increasing the coding

accuracy by reducing positively correlated noise between neurons[37]. In addition, monotonic coding allows a single neuron to encode more than one parameter using discharge rate, thereby avoiding a 'binding problem' in higher auditory areas[22]. For example, a neuron might monotonically increase or decrease its discharge rate for different stimulus parameters (such as source location and repetition rate). At the population level, if positive and negative response functions from multiple neurons are added together, the result is a flat response (invariant to the parameter). However, when similar monotonic response functions are added together, the monotonic response function is preserved. Therefore, multiple parameters can be encoded using monotonic functions of single neurons, and then a single parameter can be extracted by combining the responses of neurons with similar monotonic functions for the desired parameter, but opposite monotonic functions for all other parameters.

Potential mechanisms of unsynchronized responses

Corticocortical connections between AI, R and RT could support a cascade of temporal integration along the core's caudal-to-rostral axis. Feedforward corticocortical inputs, combined with the parallel thalamic inputs from vMGB[38] to each of the core areas, could hypothetically spread out the arrival times of inputs and decrease stimulus synchronization in R and RT relative to AI, transforming a temporal representation into a rate code. This model is supported by our observation that the rostral fields have a higher proportion of unsynchronized responses and longer peak latencies. In addition, a longer temporal integration window in unsynchronized neurons could cause the loss of stimulus-synchronized discharges in the frequency range of flutter. It has been suggested that higher levels of the auditory system analyze acoustic signals over longer time scales[39]. Whether temporal processing also differs between the caudal and rostral divisions of the non-core areas of auditory cortex (for example, the lateral belt), between core and non-core areas along the medial-to-lateral axis, or between the right and left auditory cortex[39] remains to be studied in future experiments. Our study investigated synchronized and unsynchronized responses purely from a physiological standpoint. Whether these two response types arise from morphologically distinct cell types that differ in biophysical properties or thalamocortical or corticocortical connectivity is unknown.

Perceptual effects related to temporal and rate coding

Although flutter discrimination has not been tested directly in marmosets, it has been previously shown that monkeys can discriminate between different repetition rates in the range of flutter[40,41]. Flutter perception is behaviorally relevant to marmosets, given that several of their species-specific vocalizations contain repetitive temporal patterns near or within the flutter range (for example, twitter call: ~8 Hz; trill call: ~27 Hz)[7,8]. However, to our knowledge, it has not been tested whether marmosets perceive flutter as a discrete rather than continuous sensation in the same manner as humans. A caveat to our experiments is that we are comparing physiological data obtained from marmosets with psychophysical data obtained from humans. A direct link between flutter perception and underlying neural mechanisms in the same species remains to be studied.

For both the auditory and somatosensory systems, the perceptual and neural encoding boundary for repetition rates producing a sensation of flutter (tactile and auditory) and vibration (tactile) or pitch (auditory) is around 40 Hz (refs. 4,5,13–15). In the auditory system, at least, this seems to be a direct consequence of the temporal integration window of AI neurons (~25 ms). Faster repetition rates cause multiple acoustic events to occur within the temporal integration window, and are consequently represented by the discharge rates of neurons that cannot synchronize to individual events in the stimulus[10]. With slower repetition rates, which cause a percept of flutter, only a single event occurs within the temporal integration window, so that these rates can be represented by neurons that synchronize to each event. Thus, the discrete sensation of flutter might be a direct result of synchronized responses occurring across the entire neuronal population that represents this percept. Likewise, faster repetition rates fail to sound discrete because the neurons that encode these types of sounds do not synchronize to the stimulus, and as such their discharge rates as a population do not oscillate in unison with the occurrence of each acoustic event.

It is possible that the neural responses in our study are also linked to the auditory percept of roughness, which spans the upper range of flutter and the lower range of pitch (~20–200 Hz)[42]. However, because roughness depends on other parameters (such as spectrum and envelope shape) that we did not vary in our experiments, it is premature to draw any conclusions between the neural responses we observed and the perception of roughness.

In contrast to the auditory system, the somatosensory neural populations that encode repetition rates in the perceptual range of vibration and flutter are segregated in the peripheral somatosensory system. However, potentially because the primary sensory cortices have similar temporal integration windows, the upper boundaries of the percept of flutter are similar in the two sensory systems[3,4,13]. The positive and negative monotonic unsynchronized responses observed in the rostral fields (R and RT) are similar to the neural representation of flutter observed in primate S2 (refs. 18,20). Although temporal processing in these two cortical areas might be similar, they might not be functionally homologous, given that there is a large increase in receptive field size between S1 and S2 (ref. 43) but not between AI and R[29].

In the visual system, the discrete percept of repetition rate is referred to as flicker. Although flicker is typically experienced at frequencies below 20 Hz, for high-luminance stimuli in the peripheral visual field flicker can be perceived at frequencies as high as 50–60 Hz (ref. 44). In primary visual cortex, stimulus-synchronized responses to flicker have also been observed at frequencies up to 50–60 Hz (refs. 45,46). This indicates that at least a subset of neurons in primary visual cortex can synchronize at the upper limit of flicker perception. Whether the decrease in critical flicker frequency for low luminance or foveal stimulation is the direct result of poorer stimulus synchronization has not been tested.

Perceptual and neural coding similarities for visual flicker, tactile flutter and acoustic flutter might provide a basis for cross-modal discrimination and plasticity. For instance, human subjects can discriminate between the repetition rates of a visual flicker and an acoustic flutter stimulus[47]. In addition, interval discrimination can generalize across modalities, so that subjects trained on a tactile interval discrimination task also develop improved interval discrimination for auditory stimuli (but only for similar interval durations)[48].

In a more general sense, we propose that at each cortical level of a sensory system where there is a conversion from a temporal to rate representation, there is a perceptual categorical boundary. The conversion from a temporal to rate representation in primary sensory cortex might underlie the categorical boundary between percepts of flutter and pitch (or vibration for tactile perception). Likewise, the conversion from a temporal to rate representation in non-primary sensory cortex, resulting in an overall drop in stimulus synchronization, might be responsible for determining the lower limit of flutter. Although perceptual categorical boundaries could be formed by other neural

mechanisms, we suggest that the upper and lower limit of flutter are direct results of the different temporal analysis windows used for transformations between temporal and rate coding by primary and non-primary sensory cortical areas.

METHODS

General experimental procedures. We have recently published details of experimental procedures[49]. Single-unit recordings were made using high-impedance tungsten microelectrodes (2–5 MΩ). We detected action potentials on-line using a template-matching method (MSD, Alpha Omega Engineering). All recording sessions were carried out in a double-walled, soundproof chamber (Industrial Acoustic Co., Inc.) with an interior covered by 3-inch acoustic absorption foam (Sonex, Illbruck, Inc.). Acoustic stimuli were generated digitally and delivered by a free-field speaker located 1 m directly in front of the animal. The animal was awake and semi-restrained in a custom-made primate chair, but was not performing a task during these experiments. All experimental procedures were approved by the Johns Hopkins University Animal Use and Care Committee.

Electrophysiological recordings and acoustic stimuli. After each single unit was isolated, its basic response properties (CF and sound level threshold) were measured, most commonly using pure tones or noise. Neurons located outside AI did not always respond to pure tones or noise, and for these neurons we used amplitude-modulated tones or noise to measure CF and sound level threshold. After the preferred carrier (tone or noise) and sound level were identified, we generated a set of acoustic pulse trains (each pulse was generated by windowing the preferred carrier signal by a Gaussian envelope) with repetition rates ranging from 4 to 48 Hz (in 4-Hz steps). This was the most common stimulus set (referred here to as stimulus set 1) used to test tuning for repetition rate. Another stimulus set in which the time interval between acoustic pulses was varied between 20 and 75 ms in 5- to 10-ms steps (effectively varying repetition rate between 13 and 50 Hz) was also used for a subset of neurons. If neurons could not be driven with Gaussian acoustic pulse trains, we used rectangular clicks or acoustic pulses with a ramped or damped envelope[10]. Each stimulus had a duration of 500–540 ms, depending on the width of the acoustic pulse used. Pulse widths ranged from 0.1 to 1 ms for rectangular clicks and $\sigma = 0.89$ to 4.65 ms for Gaussian pulses. All inter-trial intervals were at least 1 s long and each stimulus was presented in a randomly shuffled order with other stimuli. Each stimulus was repeated at least five times for all neurons, and at least ten times for most neurons (236/274). Stimulus intensity levels for acoustic pulse trains were generally 10–30 dB above CF-tone threshold for neurons with monotonic rate-level functions and at the preferred sound level for neurons with non-monotonic rate-level functions.

Data analysis. Neurons were considered stimulus synchronized if their vector strength was greater than 0.1 and statistically significant (Rayleigh statistic values greater than 13.8, equivalent to $P < 0.001$)[50] for at least three sequential repetition rates between 8 and 50 Hz over a span of at least 8 Hz. The vector strength was calculated over the time period starting from 50 ms after stimulus onset to 50 ms after stimulus offset. Neurons were considered to have a significant rate response if for at least three sequential repetition rates in the stimulus set (over a range of at least 8 Hz) they produced a significant discharge rate. A significant rate was defined as an average discharge rate 2 s.d. above the mean spontaneous rate, at least an average of 2 spikes per stimulus (after subtracting the mean spontaneous rate), and at least 1 spike for a minimum of 50% of the trials. We calculated average discharge rates for the duration of the stimulus plus an additional 100 ms after the stimulus.

The monotonicity of the discharge rate versus repetition rate function was determined by calculating the Spearman correlation coefficient ($P < 0.05$ for a positive or negative correlation). We calculated monotonicity over all repetition rates tested between 8 and 50 Hz. For each neuron, we also performed a linear regression on neuronal responses to repetition rates between 8 and 50 Hz, and determined whether the response slope was significantly different from zero (F-test, $P < 0.05$). We found that 179 out of 184 monotonic neurons and 16 out of 90 non-monotonic neurons had statistically significant response slopes, on the basis of this analysis.

The response slope (change in discharge rate relative to the change in repetition rate) was obtained by linear interpolation between repetition rates of 8 to 50 Hz. Individual peri-stimulus time histograms (PSTHs) were calculated by convolving a Gaussian kernel ($\sigma = 10$ ms) with a neuron's spike train. We obtained population PSTHs by taking the mean of individual PSTHs, and determined the instantaneous response slope for a neuronal population by calculating the response slope across the population PSTHs for repetition rates between 8 and 48 Hz (stimulus set 1) at a particular time. Peak latencies were computed from the population PSTH of pure tone responses (at the sound level eliciting the maximum discharge rate). A statistically significant difference in peak latencies between two neuronal populations was determined using a Wilcoxon rank sum test to compare the distribution of peak latencies obtained from individual PSTHs.

We quantified sound level invariance by linearly interpolating the response slopes at each sound level tested. The slope of this linear fit was used to estimate how much the response slope changed with a 10-dB increase in sound level. A significant difference in the sound level dependent changes of the response slopes for two populations of neurons was determined using a Kolmogorov-Smirnov test ($P < 0.05$).

Identification of cortical areas. We identified AI by its response to pure tones and cochleotopic gradient (high frequency: caudal-medial; low frequency: rostral-lateral). The rostral fields R and RT were identified by reversals in the cochleotopic gradient. The median CF of neurons that had significant responses to tones was calculated within an analysis window moving along the caudal-to-rostral axis. This was then smoothed using zero-phase forward and reverse digital filters and cochleotopic reversals were identified as minima and maxima in this curve. Although most recordings were in AI, R and RT, a subset of the neurons studied might have been in the lateral belt or parabelt. We limited our comparison of core areas to neurons within 2–2.5 mm of the lateral sulcus in regions that were generally tone-responsive. Using frequency reversals to define the borders of AI, R and RT, we created normalized maps for four hemispheres. We recorded from AI and R in two hemispheres and from AI, R and RT in the other two. We used a Wilcoxon rank sum test ($P < 0.05$) to determine whether the spatial distribution of synchronized and unsynchronized neurons was different along either the caudal-to-rostral or medial-to-lateral axis. The border area between AI and R (**Supplementary Table 1**) was defined as the 1-mm-wide region along the caudal-to-rostral axis, centered at the AI/R border.

In one monkey, we recorded from a second hemisphere; however, because it was not sufficiently mapped, we could not determine the border between AI and R, and as such the data from this hemisphere were excluded from core area comparisons ($n = 27$). In addition, we excluded 19 neurons that were identified as on the border or outside the core of auditory cortex from core area comparisons.

Note: Supplementary information is available on the Nature Neuroscience website.

ACKNOWLEDGMENTS

Support was contributed by US National Institutes of Health grants DC 03180 (X.W.) and F31 DC 006528 (D.B.). We thank A. Pistorio for assistance with animal care and Y. Zhou for valuable comments and suggestions related to this manuscript.

AUTHOR CONTRIBUTIONS

D.B. and X.W. designed the experiment and co-wrote the paper. D.B. carried out the electrophysiological recordings and data analysis.

COMPETING INTERESTS STATEMENT

The authors declare no competing financial interests.

Published online at http://www.nature.com/natureneuroscience
Reprints and permissions information is available online at http://npg.nature.com/reprintsandpermissions

1. Rosen, S. Temporal information in speech: acoustic, auditory and linguistic aspects. *Phil. Trans. R. Soc. Lond. B* **336**, 367–373 (1992).
2. Singh, N.C. & Theunissen, F.E. Modulation spectra of natural sounds and ethological theories of auditory processing. *J. Acoust. Soc. Am.* **114**, 3394–3411 (2003).
3. Miller, G.A. & Taylor, W.G. The perception of repeated bursts of noise. *J. Acoust. Soc. Am.* **20**, 171–182 (1948).

4. Besser, G.M. Some physiological characteristics of auditory flutter fusion in man. *Nature* **214**, 17–19 (1967).
5. Krumbholz, K., Patterson, R.D. & Pressnitzer, D. The lower limit of pitch as determined by rate discrimination. *J. Acoust. Soc. Am.* **108**, 1170–1180 (2000).
6. Drullman, R., Festen, J.M. & Plomp, R. Effect of reducing slow temporal modulations on speech reception. *J. Acoust. Soc. Am.* **95**, 2670–2680 (1994).
7. DiMattina, C. & Wang, X. Virtual vocalization stimuli for investigating neural representations of species-specific vocalizations. *J. Neurophysiol.* **95**, 1244–1262 (2006).
8. Pistorio, A.L., Vintch, B. & Wang, X. Acoustical analysis of vocal development in a New World primate, the common marmoset (*Callithrix jacchus*). *J. Acoust. Soc. Am.* **120**, 1655–1670 (2006).
9. Joris, P.X., Schreiner, C.E. & Rees, A. Neural processing of amplitude-modulated sounds. *Physiol. Rev.* **84**, 541–577 (2004).
10. Lu, T., Liang, L. & Wang, X. Temporal and rate representations of time-varying signals in the auditory cortex of awake primates. *Nat. Neurosci.* **4**, 1131–1138 (2001).
11. Lu, T. & Wang, X. Information content of auditory cortical responses to time-varying acoustic stimuli. *J. Neurophysiol.* **91**, 301–313 (2004).
12. Bieser, A. & Muller-Preuss, P. Auditory responsive cortex in the squirrel monkey: neural responses to amplitude-modulated sounds. *Exp. Brain Res.* **108**, 273–284 (1996).
13. Talbot, W.H., Darian-Smith, I., Kornhuber, H.H. & Mountcastle, V.B. The sense of flutter-vibration: comparison of the human capacity with response patterns of mechanoreceptive afferents from the monkey hand. *J. Neurophysiol.* **31**, 301–334 (1968).
14. Wang, X., Lu, T. & Liang, L. Cortical processing of temporal modulations. *Speech Commun.* **41**, 107–121 (2003).
15. Mountcastle, V.B., Talbot, W.H., Darian-Smith, I. & Kornhuber, H.H. Neural basis of the sense of flutter-vibration. *Science* **155**, 597–600 (1967).
16. Mountcastle, V.B., Talbot, W.H., Sakata, H. & Hyvarinen, J. Cortical neuronal mechanisms in flutter-vibration studied in unanesthetized monkeys. Neuronal periodicity and frequency discrimination. *J. Neurophysiol.* **32**, 452–484 (1969).
17. Mountcastle, V.B., Steinmetz, M.A. & Romo, R. Frequency discrimination in the sense of flutter: psychophysical measurements correlated with postcentral events in behaving monkeys. *J. Neurosci.* **10**, 3032–3044 (1990).
18. Salinas, E., Hernandez, A., Zainos, A. & Romo, R. Periodicity and firing rate as candidate neural codes for the frequency of vibrotactile stimuli. *J. Neurosci.* **20**, 5503–5515 (2000).
19. Luna, R., Hernandez, A., Brody, C.D. & Romo, R. Neural codes for perceptual discrimination in primary somatosensory cortex. *Nat. Neurosci.* **8**, 1210–1219 (2005).
20. Romo, R. & Salinas, E. Flutter discrimination: neural codes, perception, memory and decision making. *Nat. Rev. Neurosci.* **4**, 203–218 (2003).
21. McAlpine, D., Jiang, D. & Palmer, A.R. A neural code for low-frequency sound localization in mammals. *Nat. Neurosci.* **4**, 396–401 (2001).
22. Stecker, G.C., Harrington, I.A. & Middlebrooks, J.C. Location coding by opponent neural populations in the auditory cortex. *PLoS Biol.* **3**, e78 (2005).
23. Leopold, D.A., Bondar, I.V. & Giese, M.A. Norm-based face encoding by single neurons in the monkey inferotemporal cortex. *Nature* **442**, 572–575 (2006).
24. Butts, D. & Goldman, M. Tuning curves, neuronal variability, and sensory coding. *PLoS Biol.* **4**, e92 (2006).
25. Salinas, E. How behavioral constraints may determine optimal sensory representations. *PLoS Biol.* **4**, e387 (2006).
26. Kaas, J.H. & Hackett, T.A. Subdivisions of auditory cortex and processing streams in primates. *Proc. Natl. Acad. Sci. USA* **97**, 11793–11799 (2000).
27. Petkov, C.I., Kayser, C., Augath, M. & Logothetis, N.K. Functional imaging reveals numerous fields in the monkey auditory cortex. *PLoS Biol.* **4**, e215 (2006).
28. Morel, A. & Kaas, J.H. Subdivisions and connections of auditory cortex in owl monkeys. *J. Comp. Neurol.* **318**, 27–63 (1992).
29. Recanzone, G.H., Guard, D.C. & Phan, M.L. Frequency and intensity response properties of single neurons in the auditory cortex of the behaving macaque monkey. *J. Neurophysiol.* **83**, 2315–2331 (2000).
30. Rauschecker, J.P., Tian, B. & Hauser, M. Processing of complex sounds in the macaque nonprimary auditory cortex. *Science* **268**, 111–114 (1995).
31. Barbour, D.L. & Wang, X. Contrast tuning in auditory cortex. *Science* **299**, 1073–1075 (2003).
32. Pollack, I. Discrimination of mean temporal interval within jittered auditory pulse trains. *J. Acoust. Soc. Am.* **43**, 1107–1112 (1968).
33. Bendor, D. & Wang, X. The neuronal representation of pitch in primate auditory cortex. *Nature* **436**, 1161–1165 (2005).
34. Pollack, I. Auditory random-walk discrimination. *J. Acoust. Soc. Am.* **46**, 422–425 (1969).
35. Brugge, J.F. & Merzenich, M.M. Responses of neurons in auditory cortex of the macaque monkey to monaural and binaural stimulation. *J. Neurophysiol.* **36**, 1138–1158 (1973).
36. Polley, D.B., Heiser, M.A., Blake, D.T., Schreiner, C.E. & Merzenich, M.M. Associative learning shapes the neural code for stimulus magnitude in primary auditory cortex. *Proc. Natl. Acad. Sci. USA* **101**, 16351–16356 (2004).
37. Romo, R., Hernandez, A., Zainos, A. & Salinas, E. Correlated neuronal discharges that increase coding efficiency during perceptual discrimination. *Neuron* **38**, 649–657 (2003).
38. Rauschecker, J.P., Tian, B., Pons, T. & Mishkin, M. Serial and parallel processing in rhesus monkey auditory cortex. *J. Comp. Neurol.* **382**, 89–103 (1997).
39. Boemio, A., Fromm, S., Braun, A. & Poeppel, D. Hierarchical and asymmetric temporal sensitivity in human auditory cortices. *Nat. Neurosci.* **8**, 389–395 (2005).
40. Moody, D.B. Detection and discrimination of amplitude-modulated signals by macaque monkeys. *J. Acoust. Soc. Am.* **95**, 3499–3510 (1994).
41. Beitel, R.E., Schreiner, C.E., Cheung, S.W., Wang, X. & Merzenich, M.M. Reward-dependent plasticity in the primary auditory cortex of adult monkeys trained to discriminate temporally modulated signals. *Proc. Natl. Acad. Sci. USA* **100**, 11070–11075 (2003).
42. Fishman, Y.I., Reser, D.H., Arezzo, J.C. & Steinschneider, M. Complex tone processing in primary auditory cortex of the awake monkey. I. Neural ensemble correlates of roughness. *J. Acoust. Soc. Am.* **108**, 235–246 (2000).
43. Fitzgerald, P.J., Lane, J.W., Thakur, P.H. & Hsiao, S.S. Receptive field (RF) properties of the macaque second somatosensory cortex: RF size, shape, and somatotopic organization. *J. Neurosci.* **26**, 6485–6495 (2006).
44. Hartmann, E., Lachenmayr, B. & Brettel, H. The peripheral critical flicker frequency. *Vision Res.* **19**, 1019–1023 (1979).
45. Rager, G. & Singer, W. The response of cat visual cortex to flicker stimuli of variable frequency. *Eur. J. Neurosci.* **10**, 1856–1877 (1998).
46. Williams, P.E., Mechler, F., Gordon, J., Shapley, R. & Hawken, M.J. Entrainment to video displays in primary visual cortex of macaque and humans. *J. Neurosci.* **24**, 8278–8288 (2004).
47. Gebhard, J.W. & Mowbray, G.H. On discriminating the rate of visual flicker and auditory flutter. *Am. J. Psychol.* **72**, 521–529 (1959).
48. Nagarajan, S.S., Blake, D.T., Wright, B.A., Byl, N. & Merzenich, M.M. Practice-related improvements in somatosensory interval discrimination are temporally specific but generalize across skin location, hemisphere, and modality. *J. Neurosci.* **18**, 1559–1570 (1998).
49. Liang, L., Lu, T. & Wang, X. Neural representations of sinusoidal amplitude and frequency modulations in the primary auditory cortex of awake primates. *J. Neurophysiol.* **87**, 2237–2261 (2002).
50. Mardia, K.V. & Jupp, P.E. *Directional Statistics* (John Wiley & Sons, New York, 2000).

Supplementary Table 1 (Bendor and Wang 2007)

	AI	Rostral fields	R	RT	AI without border	AI/R border	Rostral fields without border	Outside core	Unmapped hemisphere	Total
Sync +	26	5	4	1	20	9	2	0	3	34
Sync -	16	14	10	4	15	2	13	2	1	33
Sync M	43	19	14	5	36	11	15	2	4	68
Sync NM	21	13	10	3	16	7	11	2	3	39
Sync total	64	32	24	8	52	18	26	4	7	107
Unsync +	19	34	23	11	13	15	25	1	7	61
Unsync -	2	19	15	4	1	4	16	7	2	30
Unsync M	21	53	38	15	14	19	41	8	9	91
Unsync NM	15	20	16	4	8	9	18	5	7	47
Unsync total	36	73	54	19	22	28	59	13	16	138
Mixed +	5	5	4	1	4	3	3	0	3	13
Mixed -	3	4	3	1	2	1	4	2	0	9
Mixed M	9	10	8	2	7	4	8	2	4	25
Mixed NM	2	2	1	1	1	1	2	0	0	4
Mixed total	11	12	9	3	8	5	10	2	4	29
Total	111	117	87	30	82	51	95	19	27	274

Sync: synchronized units **Unsync: unsynchronized units**
M: monotonic units **NM: non-monotonic units**
+: positive monotonic **- : negative monotonic**

Supplementary Table 1: Number of neurons for each response type by cortical region

AI, R, and RT are defined based on frequency reversals in the cochleotopic map. The rostral fields consist of both field R and RT. The border region between AI and R is centered at the low frequency reversal, and extends 0.5 mm along the caudal-to-rostral axis each way (total width is 1 mm).

Supplementary figure S1 (Bendor and Wang 2007)

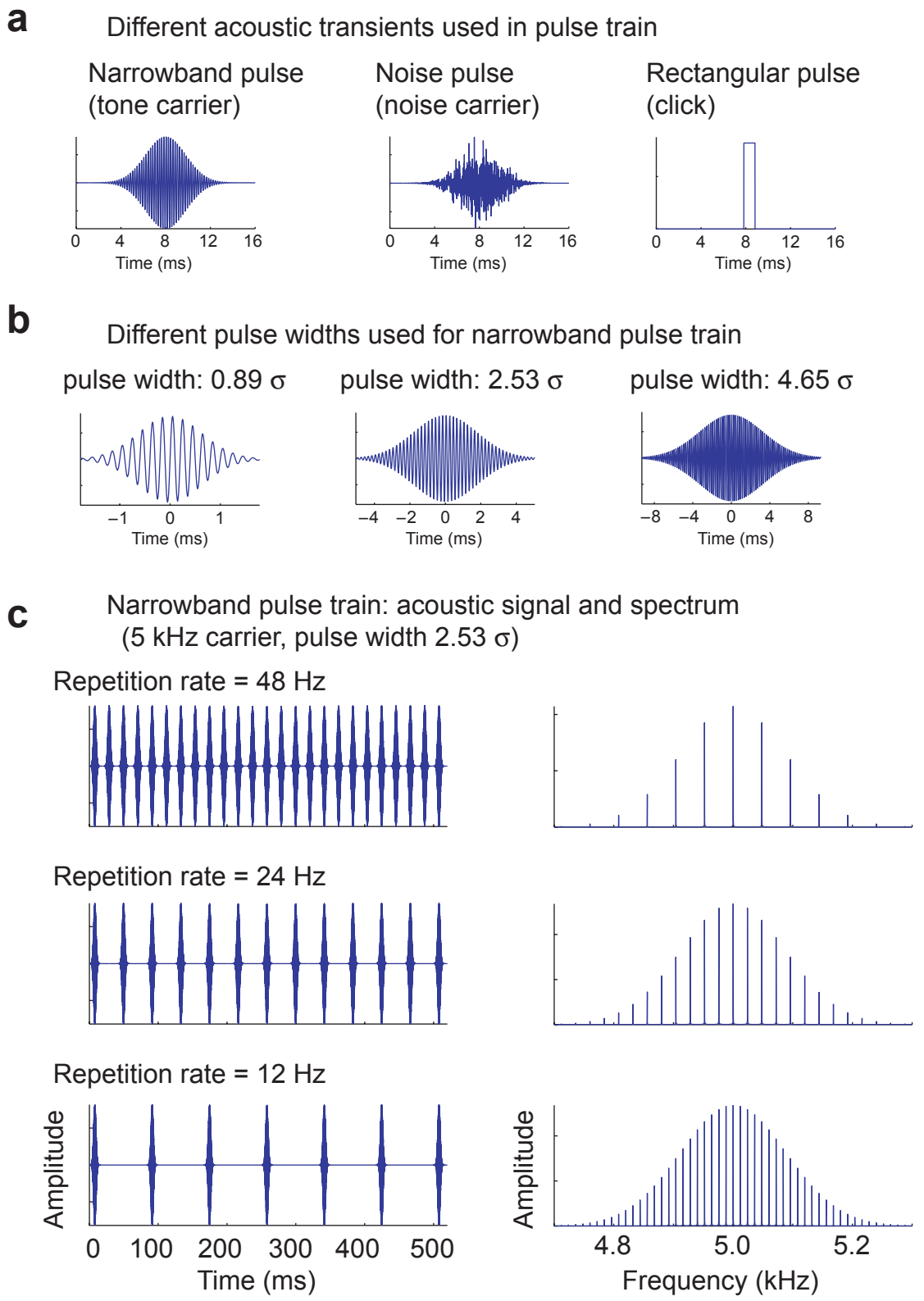

Supplementary Figure S1: Description of acoustic stimulus set

a. Three different acoustic transients used in the generation of pulse trains (tone, noise, rectangular click).

b. Range of pulse widths used in generating acoustic transients (2.53 s was the most common).

c. Example of the acoustic signal and spectrum of three acoustic pulse trains (repetition rate=12, 24, 48 Hz)

Supplementary figure S2 (Bendor and Wang 2007)

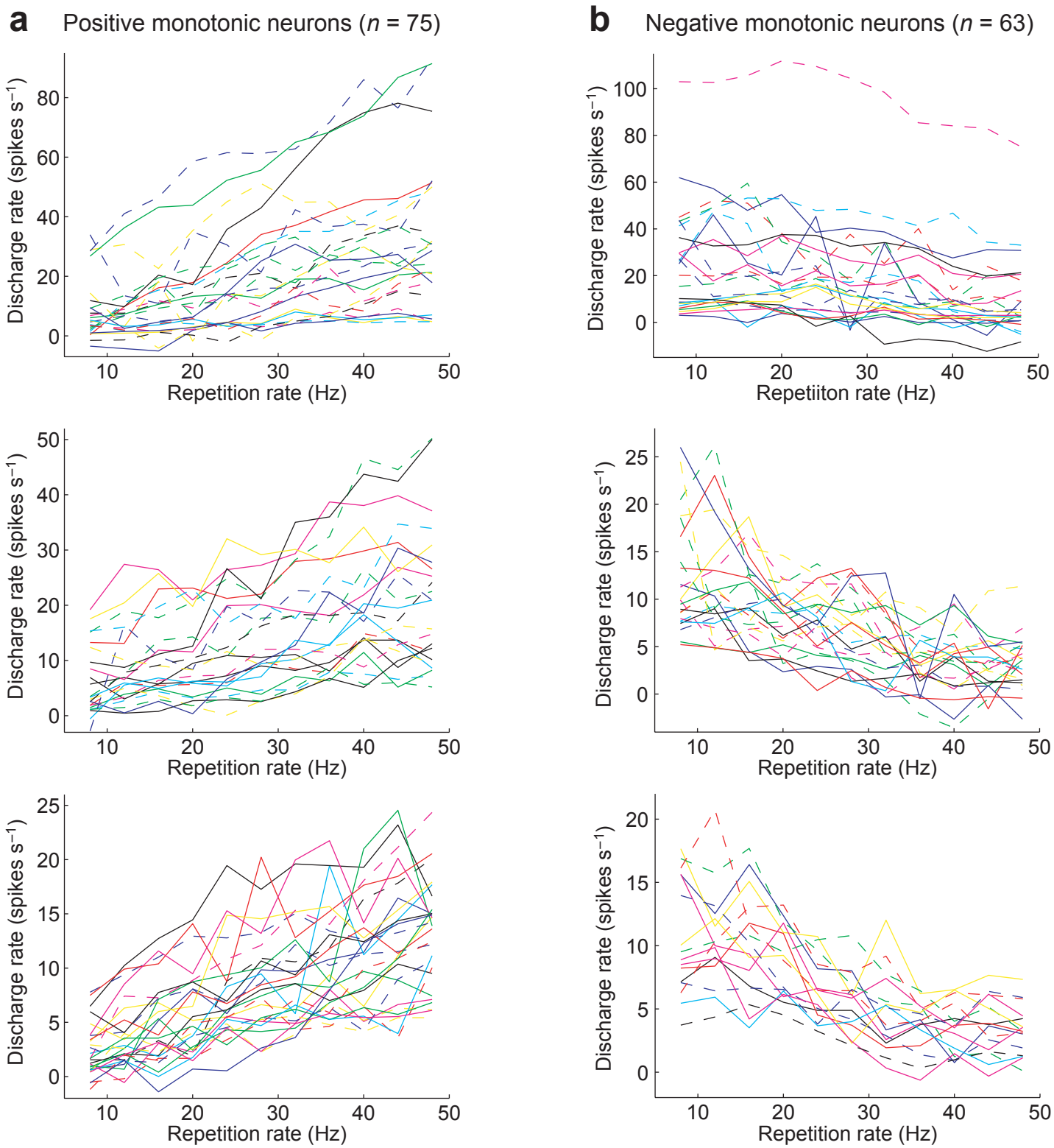

Supplementary Figure S2: Individual monotonic responses
Responses of all positive (**a**) and negative (**b**) monotonic neurons used in **Fig. 2b**. The entire range of repetition rates used to calculate the Spearman correlation coefficient is displayed (8–48 Hz). Multiple plots, line colors and types (dashed, solid) are used only for the purpose of visual clarity.

Supplementary figure S3 (Bendor and Wang 2007)

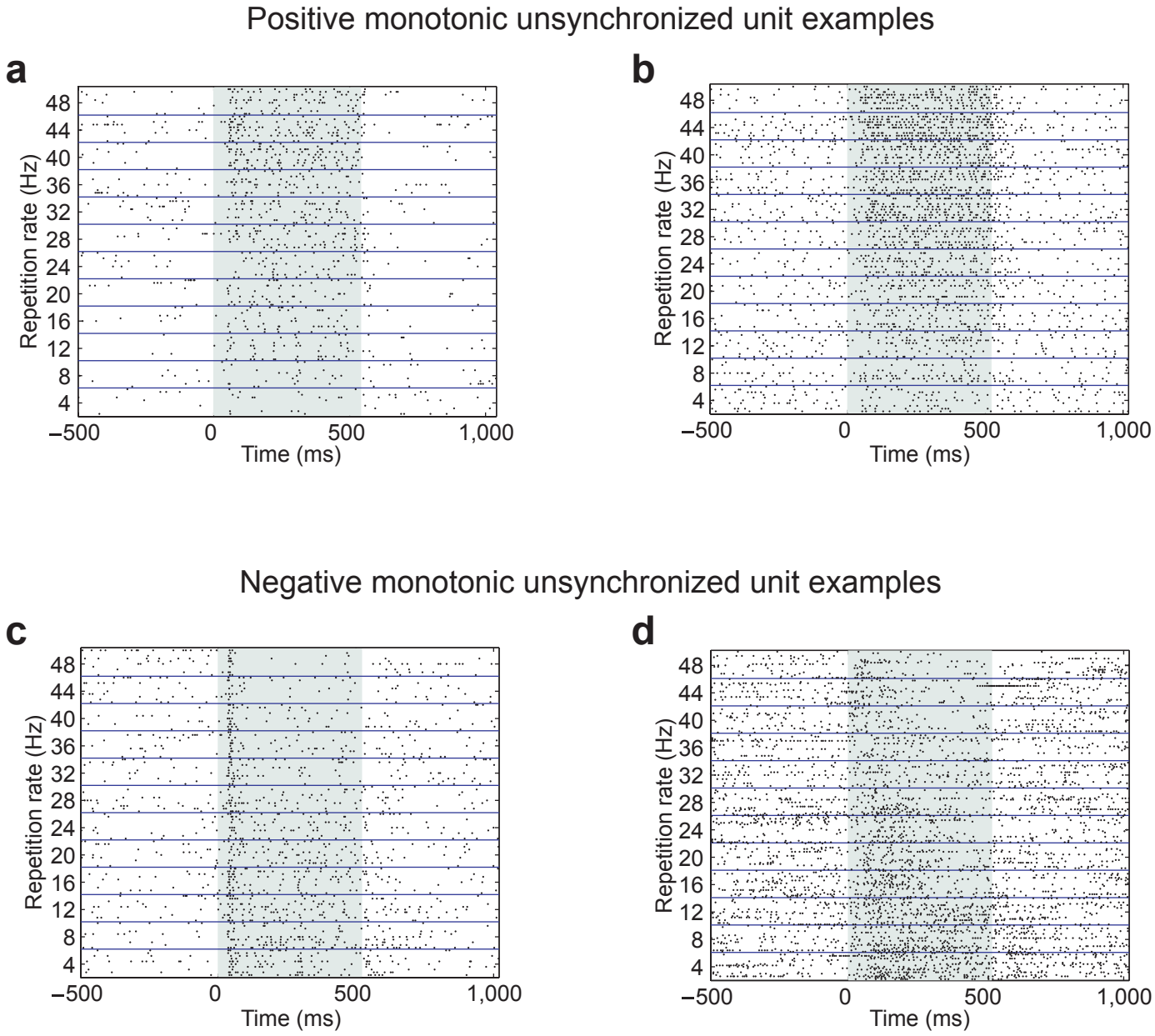

Supplementary Figure S3: Additional examples of monotonic unsynchronized neurons
Raster plot of monotonic pulse train responses for unsynchronized neurons. The shaded portion of the plot indicates the time period when the acoustic stimulus was played:

a. Unit M41O-294 (positive monotonic), significant stimulus synchronization for an 8 and 12 Hz repetition rate only

b. Unit M2P-921 (positive monotonic), no significant stimulus synchronization

c. Unit M2P-287 (negative monotonic), significant stimulus synchronization for a 4 Hz repetition rate only

d. Unit M32Q-142 (negative monotonic), no significant stimulus synchronization

Supplementary figure S4 (Bendor and Wang 2007)

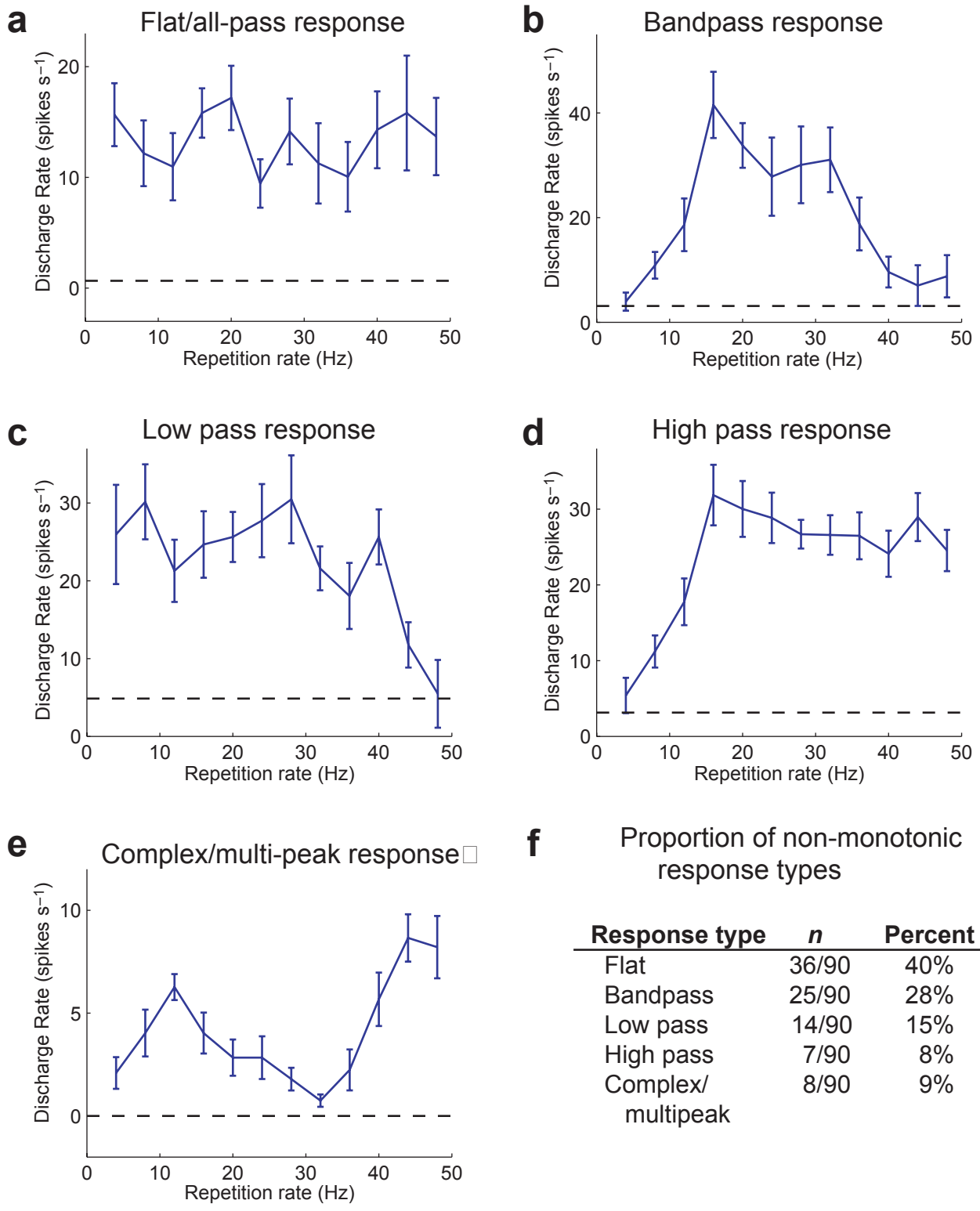

f Proportion of non-monotonic response types

Response type	*n*	Percent
Flat	36/90	40%
Bandpass	25/90	28%
Low pass	14/90	15%
High pass	7/90	8%
Complex/ multipeak	8/90	9%

Supplementary Figure S4: Single neuron examples of non-monotonic responses

a. Flat or all pass response (unit M32Q-226)
b. Band pass response (unit M2P-438)
c. Low pass response (unit M2P-338)
d. High pass response (unit M41O-262)
e. Complex/multi-peak response (unit M32Q-42)
f. Proportion of each non-monotonic response type

Supplementary figure S5 (Bendor and Wang 2007)

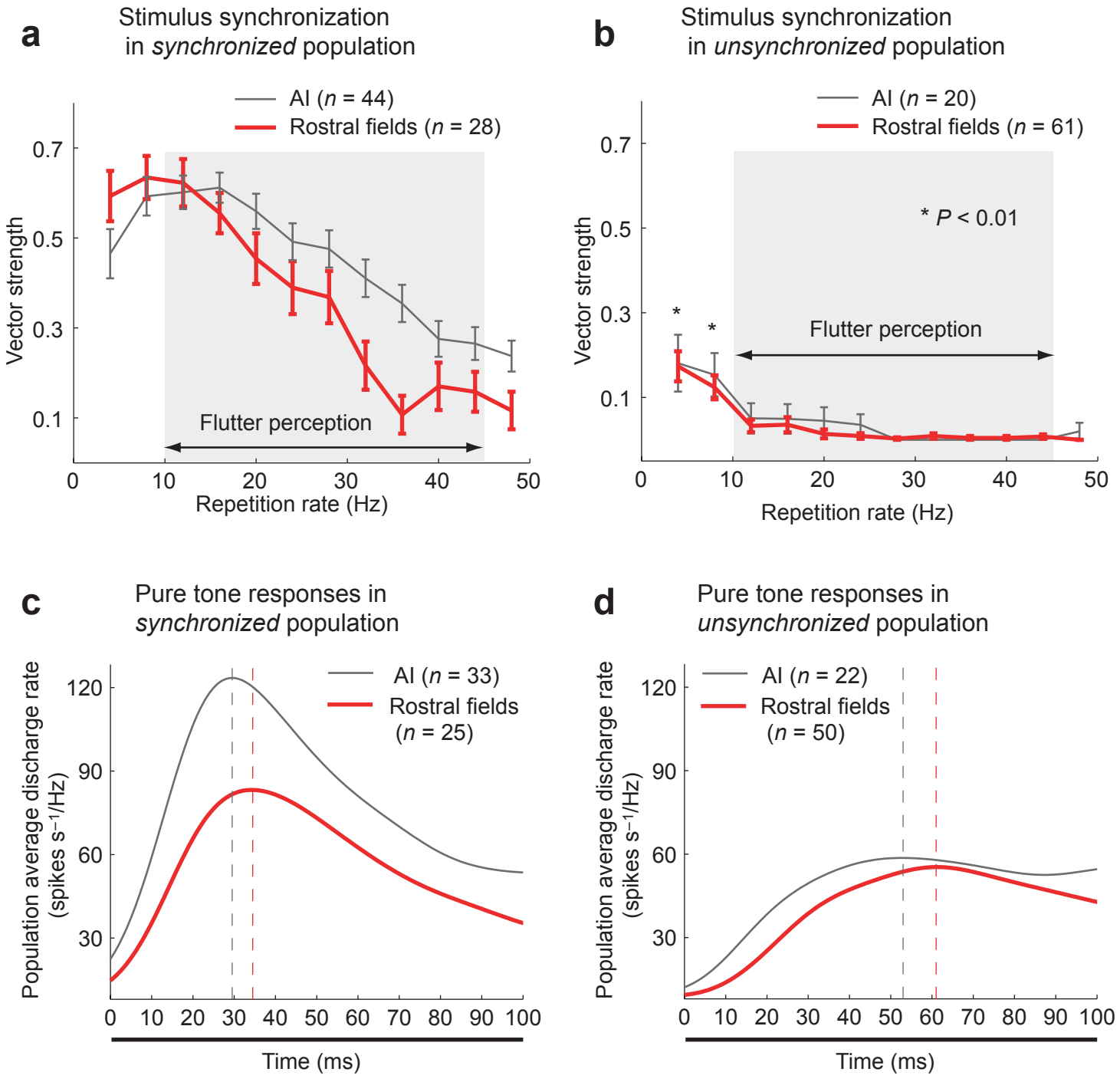

Supplementary Figure S5: Area comparison of stimulus synchronization and peak response latencies

a. Average vector strength of synchronized neurons in AI (gray) and the rostral fields (red). Both populations had significant vector strengths over the entire range of flutter (Wilcoxon rank sum test, $P < 0.01$).

b. Average vector strength of unsynchronized neurons in AI (gray) and the rostral fields (red). Both populations had significant vector strengths only for repetition rates of 4 and 8 Hz (Wilcoxon rank sum test, $P < 0.01$).

c-d. Population PSTH of (c) synchronized and (d) unsynchronized neurons in AI (gray) and the rostral fields (red) for a pure tone at the sound level eliciting the maximum discharge rate. The dashed lines indicate the peak latencies of neurons in AI (gray) and the rostral fields (red).

Supplementary figure S6 (Bendor and Wang 2007)

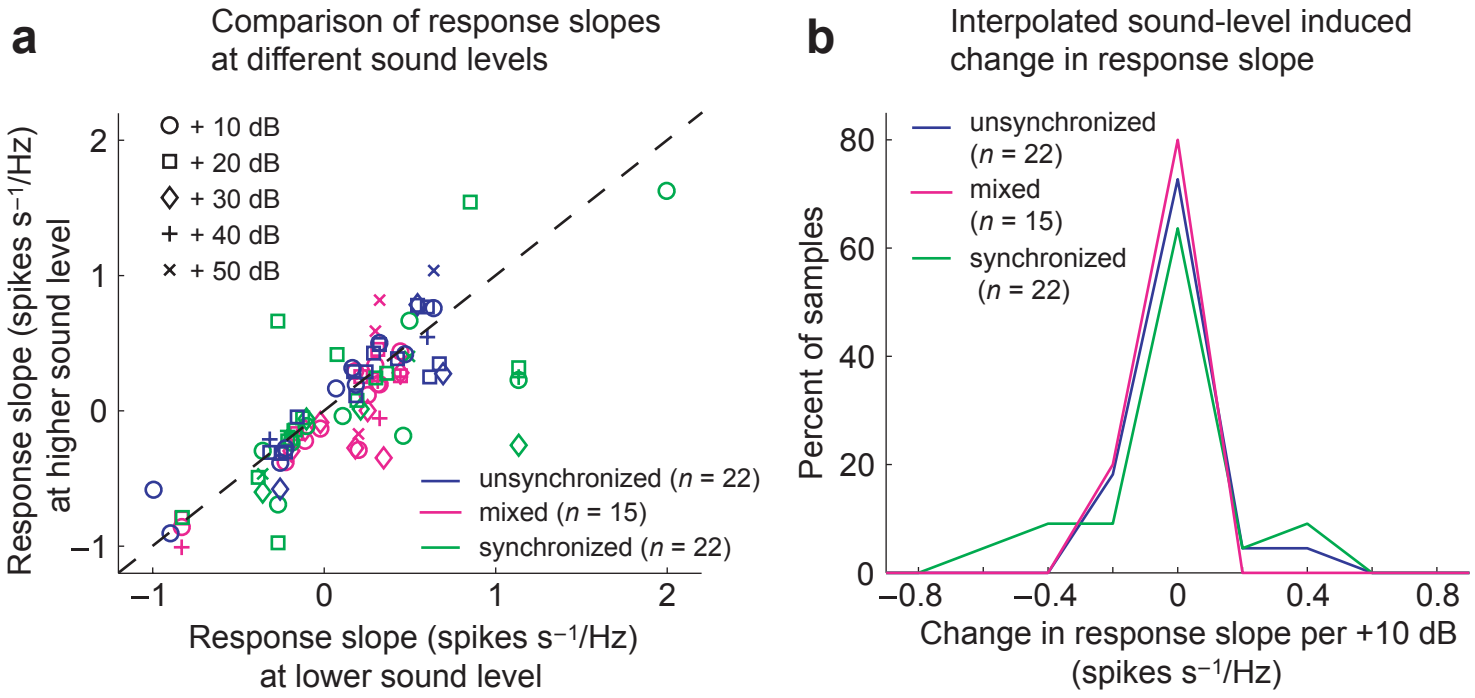

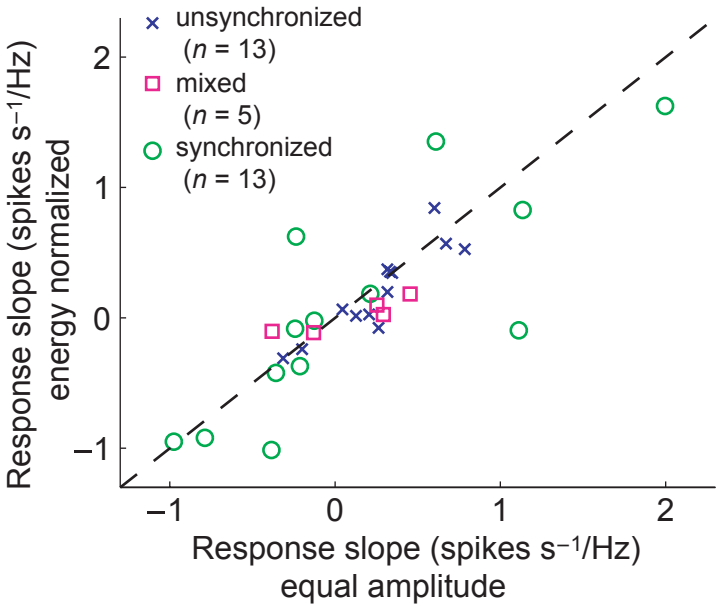

Supplementary Figure S6: Sound level dependent changes in the response slopes of monotonic neurons

a. Comparison of the response slope for monotonic synchronized (green), mixed (purple), and unsynchronized (blue) neurons at the minimum sound level producing a significant discharge rate (*x*-axis) and a sound level 10 to 50 dB higher (*y*-axis). The Pearson correlation coefficients (and *P* values) of the data were: unsynchronized ($r = 0.90$, $P < 7.7 \times 10^{-9}$), synchronized ($r = 0.78$, $P < 1.8 \times 10^{-5}$), mixed ($r = 0.83$, $P < 1.6 \times 10^{-4}$). The diagonal dashed line has a slope of 1.

b. The change in response slope for a 10 dB increase in sound level for monotonic synchronized (green), mixed (purple), and unsynchronized (blue) neurons. The distributions were not significantly different (Kolmogorov-Smirnov test, $P > 0.1$).

c. Comparison of the response slope for monotonic synchronized (green), mixed (purple), and unsynchronized (blue) neurons for energy normalized and equal amplitude pulse trains. The Pearson correlation coefficients and *P* values of the data were: unsynchronized ($r = 0.90$, $P < 3.3 \times 10^{-5}$), synchronized ($r = 0.81$, $P < 9.0 \times 10^{-4}$), mixed ($r = 0.91$, $P < 0.03$). The linear fits of the data ($y = ax + b$) were: unsynchronized ($b = 0.95$, $a = -0.05$), synchronized ($b = 0.80$, $a = -0.05$), and mixed ($b = 0.34$, $a = -0.02$). The diagonal dashed line has a slope of 1.